Available online at www.sciencedirect.com

ScienceDirect

Ceramics International 40 (2014) 2275–2280

CERAMICS INTERNATIONAL

www.elsevier.com/locate/ceramint

Hollow Zn_2SnO_4 boxes coated with N-doped carbon for advanced lithium-ion batteries

Yang Zhao, Ying Huang*, Qiufen Wang, Ke Wang, Meng Zong, Lei Wang, Xu Sun

Department of Applied Chemistry and The Key Laboratory of Space Applied Physics and Chemistry, Ministry of Education, School of Science, Northwestern Polytechnical University, Xi'an 710072, PR China

Received 2 July 2013; received in revised form 3 July 2013; accepted 30 July 2013
Available online 19 August 2013

Abstract

Hollow Zn_2SnO_4@N–C composites were synthesized after the calcined process of precursor. The N-doped carbon coating layers, as a physical buffering matrix to reinforce the hollow structure, prevent interparticle agglomeration and improve the electronic conductivity of the electrodes. Compared with our previous studies, Zn_2SnO_4@N–C composites show an enhanced electrochemical performance (616 mA h g^{-1} after 45 cycles) and high rate capability. With rational and delicate design, this kind of composites may be the potential anode materials for lithium-ion batteries.

Keywords: Hollow boxes; N-doped carbon coating; Lithium-ion batteries; Electrochemical properties; Anode materials

1. Introduction

High capacity has become an important feature of electrical storage devices, but is subject to dramatic reductions in most rechargeable batteries [1]. As one of the most important energy-storage devices, lithium-ion batteries have attracted much attention in the scientific and industrial fields [2–5]. Despite its many advantages over other competing energy storage technologies, there is a plenty of room for improvements in terms of power rate, cycle performance, and safety [6–8]. The development of new electrode materials is a key factor to improve the property of lithium-ion batteries [9,10]. At present, graphite is widely used as an anode material for lithium ion batteries, but its relatively low theoretical capacity (372 mA h g^{-1}) limits further applications [11–14].

$MSnO_3$ or $MSnO_4$ materials, as possible metal oxides anodes, attract researchers' much attention for higher reversible capacities, low cost, easy preparation and especially various morphologies [15–19]. In addition, Zn_2SnO_4 have drawn more attention as anode materials for lithium-ion batteries [20–23]. In our previous studies, the monodispersed hollow Zn_2SnO_4 boxes without impurity particles or aggregates had been synthesized by the simple co-precipitation and alkali etching way [24]. The hollow boxes display an electrochemical performance with high capacity and good cycling stability than the solid cubes and those reported. However, they also suffer from poor cycling performance owing to large specific volume changes, pretty low electronic conductivity, nanoparticle aggregation during Li insertion/extraction processes [25–28]. Conductive materials coating layers on the surface could improve the surface conductivity and the electrical contact in the electrode and buffer the volume change. Several methods of surface modification on Zn_2SnO_4 have been developed to increase its electrical conductivity, electrical contact and alleviate the volume expansion, such as using highly conductive carbon, graphene or conductive polymer [29,30].

In this work, 1-methylimidazole, as a kind of liquid nitrogen-containing organic compounds, was used as a carbon precursor to form a conducting network in hollow Zn_2SnO_4 boxes for the first time. 1-Methylimidazole was used as new precursors to obtain N-doped graphitized carbon [31–33]. Compared with conventional carbon precursors, 1-methylimidazole can penetrate

*Corresponding author. Tel.: +86 29 88431636.
E-mail addresses: zhaoyang890@163.com (Y. Zhao), yingh@nwpu.edu.cn (Y. Huang).

0272-8842/$ - see front matter © 2013 Elsevier Ltd and Techna Group S.r.l. All rights reserved.
http://dx.doi.org/10.1016/j.ceramint.2013.07.147

into porous materials easily, because of it fluidic properties. This is favorable for forming a thin carbon coating layer on the surface of boxes. Thus, using a liquid 1-methylimidazole as precursors has a significant advantage in tuning the composition and properties of the coating layer and the interphase, which is essential for material design and optimization [30].

2. Experimental

2.1. Sample preparation

Hollow $ZnSn(OH)_6$ boxes were prepared via a simple co-precipitation and alkali etching method based on our previous study [24]. The 1-methylimidazole was chosen as the precursor, which is composed of only C, N, and H elements. 400 μL of 1-methylimidazole were mixed with $ZnSn(OH)_6$ powder (0.8 g) and then the mixtures were heated at 600 °C in Ar atmosphere

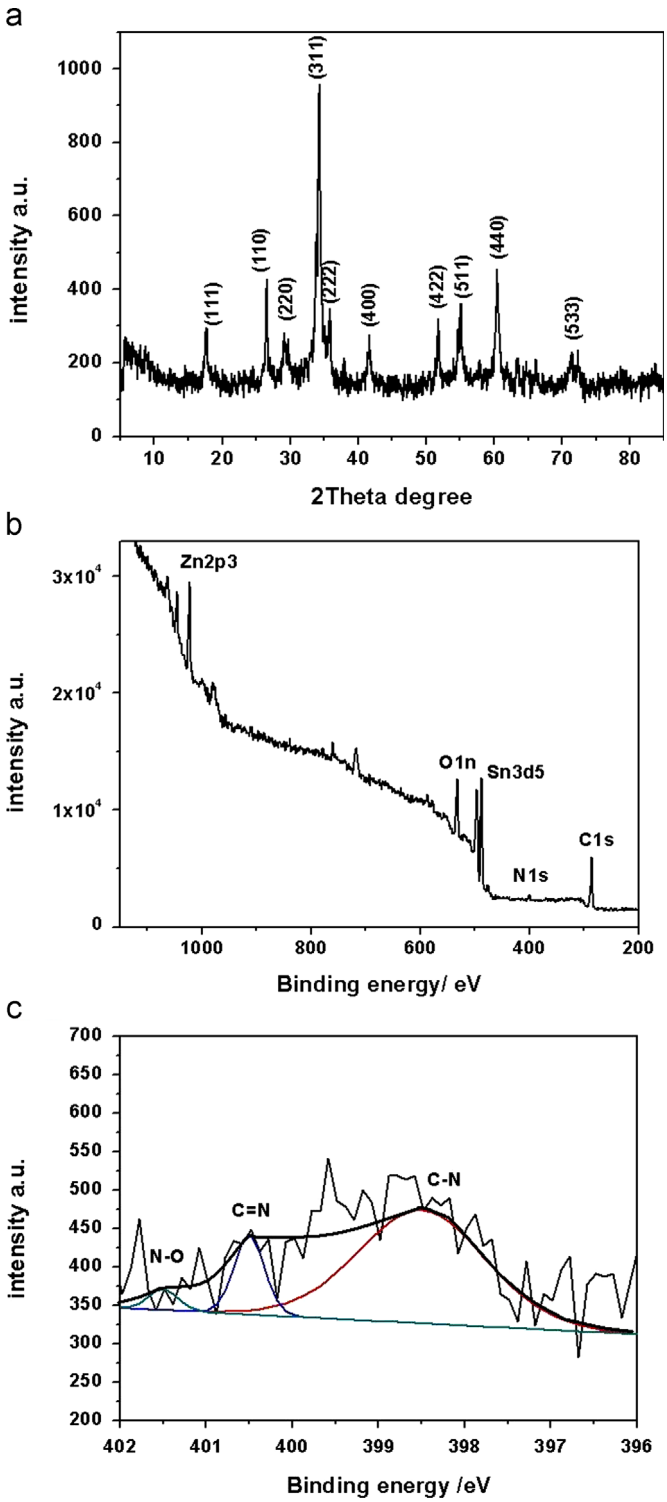

Fig. 1. (a) XRD pattern of the Zn_2SnO_4@N–C composites; (b) XPS survey spectra of the Zn_2SnO_4@N–C composites; and (c) high resolution XPS spectrum of N 1s in the Zn_2SnO_4@N–C composites.

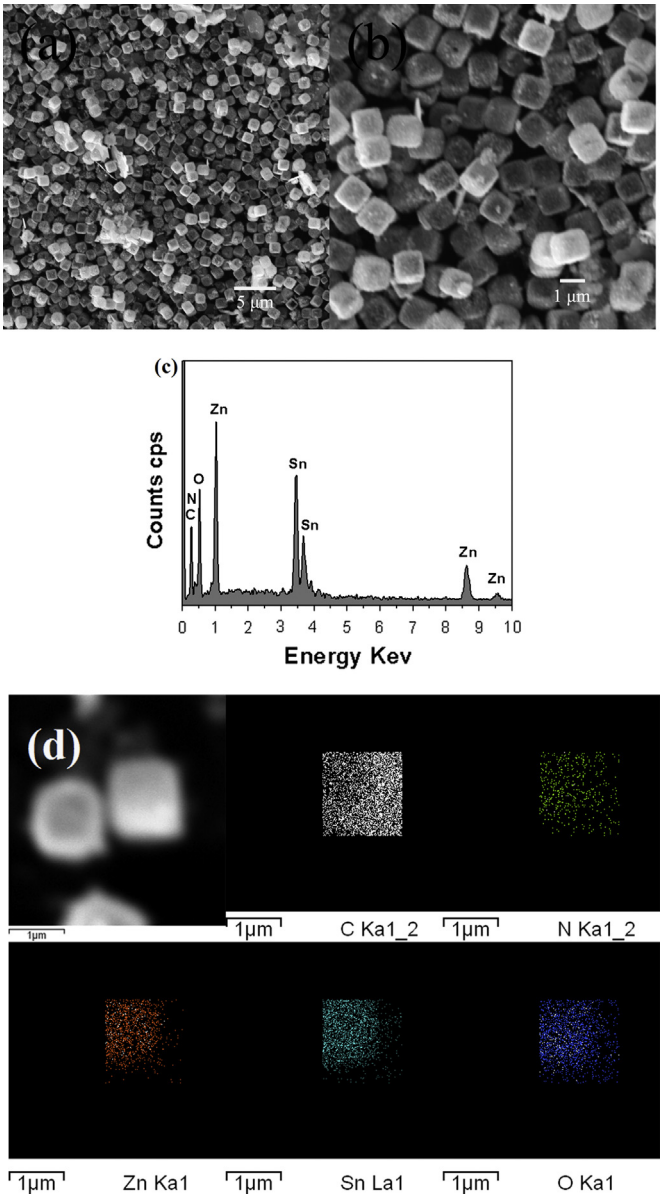

Fig. 2. (a and b) SEM and images of Zn_2SnO_4@N–C composites; (c) EDX spectrum of Zn_2SnO_4@C composites; and (d) elemental mapping showing the homogeneous distribution of all three elements of N, C, Sn, Zn and O in the composite.

for 3 h. The Zn_2SnO_4@N–C composites were obtained after the sintering process.

2.2. Materials characterization

X-ray diffraction analysis (XRD) (Rigaku, model D/max-2500 system at 40 kV and 100 mA of Cu Kα) was employed to characterize structures of the prepared samples. The surface morphology of the composites were performed by model Tecnai F30 G2 (FEI CO, USA) field emission transmission electron microscope (FETEM) and scanning electron microscope (SEM, VEGA 3, The Czech Republic, TESCAN).

We used a multi-channel current static system Land (LAND CT200IA) to evaluate the electrochemical performance of a CR2016-type coin cell. The anode electrodes prepared consist of Zn_2SnO_4@N–C (65 wt%) with acetylene black (15 wt%) and PVDF (20 wt%) as a binder dissolved in 1-methyl-2-pyrrolidinone (NMP) solution on a copper foil. Li foil was used as counter electrode, polypropylene (PP) film (Celgard 2400) as separator. The electrolyte was a solution of 1 M $LiPF_6$ in a mixture of ethylene (EC), dimethyl carbonate (DMC) and diethyl carbonate (DEC) (1:1:1, v/v/v).

3. Results and discussion

Fig. 1a shows the XRD pattern of the Zn_2SnO_4@N–C composites. The diffraction patterns of Zn_2SnO_4@N–C composites match well with the standard data of Zn_2SnO_4 cubic crystal structure, which the lattice constants is $a=8.657$ Å, $b=8.657$ Å, and $c=8.657$ Å (PDF# 24-1470). The peaks of the N-doped carbon have not been obviously observed due to the little content and the non-crystalline structure of it.

The XPS survey spectrum of Zn2SnO4@N–C composites is shown in Fig. 2b. The peaks at about 399 eV and 285 eV correspond to N 1s and C 1s, indicating the presence of N and C in the coating layer. Typical high-resolution XPS spectrum of N 1s for the composites is shown in Fig. 2c. There are there peaks at around 398.5, 400.5, and 401.5 eV can be attributed to the C–N, C═N, and N–O bonds, respectively. The existence of different C–N bonds indicates different configurations of N-doped carbon: pyridine-like nitrogen with a C–N bond together with a C═N bond and graphite-like nitrogen with three C–N bonds [30].

The structure of hollow Zn_2SnO_4 boxes provides the ability of exploiting coating of amorphous N-doping carbon around the particle by sintering of N-containing organic compounds. The

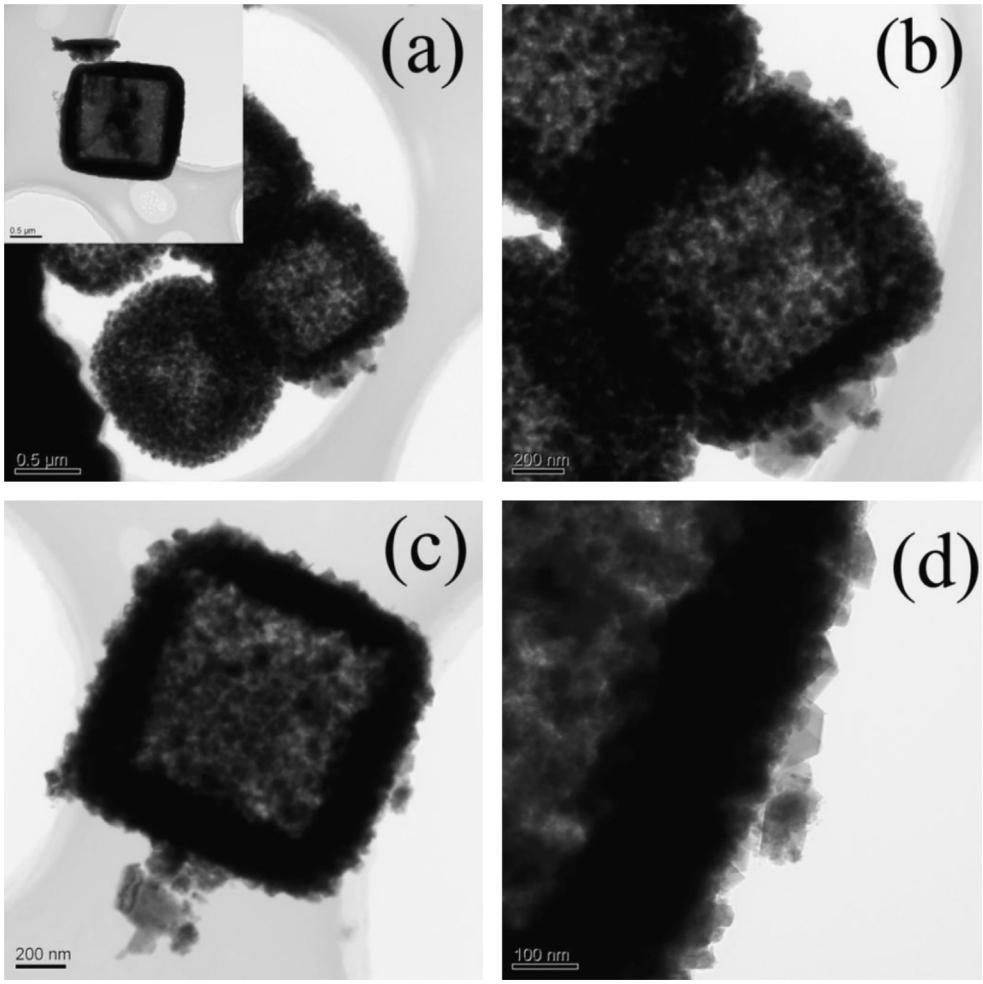

Fig. 3. TEM images of Zn_2SnO_4@C composites (a, b, c, d).

SEM images of Zn_2SnO_4@N–C composites are shown in Fig. 2a and b. After N-doping carbon coating, there is no apparent change in the box structure although their surface becomes slightly rougher. From Fig. 2b, granular carbon particles distribute on the surface of boxes to form the thin carbon coating layer. The EDS measurement confirms the co-existence of Zn, Sn, O, C and N elements (Fig. 2c). From the results of EDS analysis, the mass fraction of N element in the composites is about 5.53%. It demonstrates that N is effectively retained in the carbon coating layers after the sintering of 1-methylimidazole. The elemental mapping evidences the distribution of all elements within the composites, which is shown in Fig. 2d. It shows that N elements appear with the emergence of C elements.

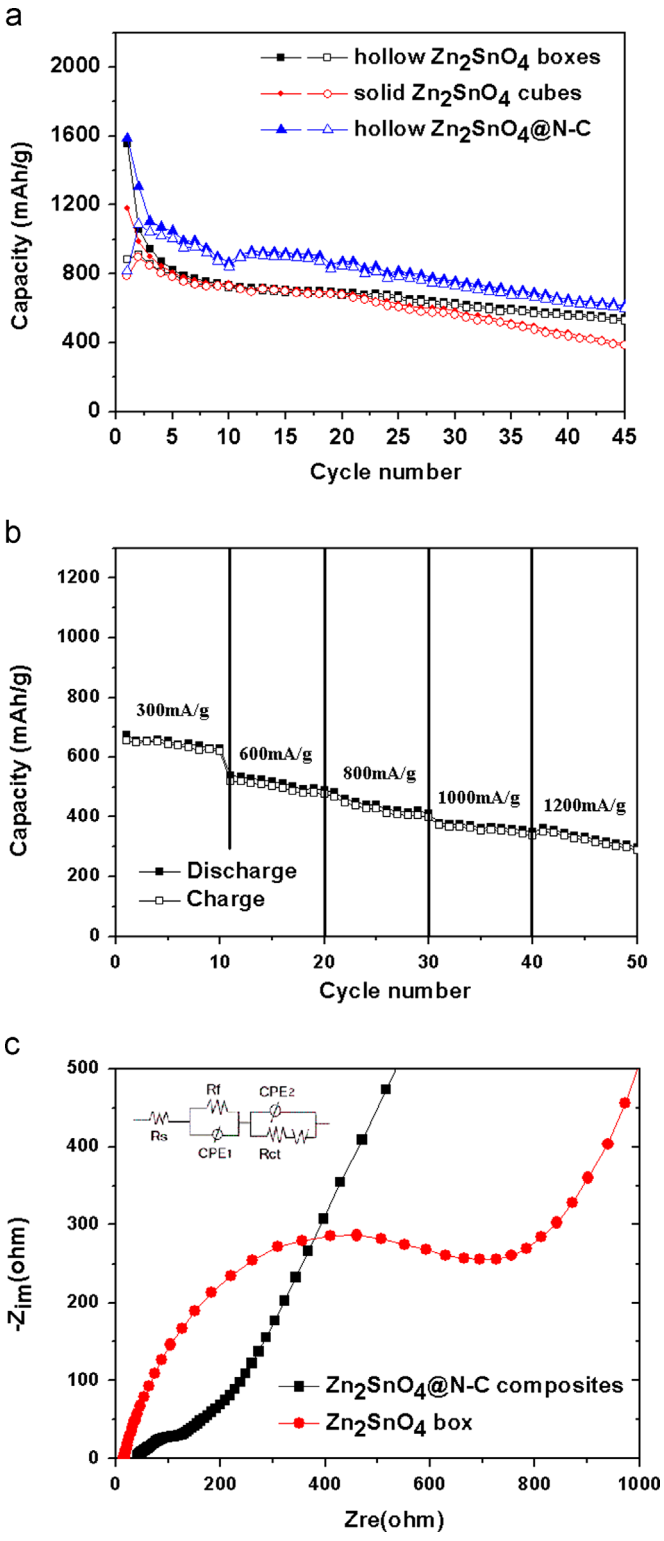

Fig. 4. (a) comparative cycling performance of Zn_2SnO_4@N–C composites, hollow Zn_2SnO_4 boxes and Zn_2SnO_4 cubes; these tests are conducted at a current density of 300 mA g^{-1} between 0.01 and 2.0 V; (b) rate capability of hollow Zn_2SnO_4 boxes which is obtained between 0.01 and 2.0 V at various current densities; and (c) EIS of the Zn_2SnO_4@N–C composites and hollow Zn_2SnO_4 boxes, including the equivalent circuit model of the studied system.

Fig. 3 shows the TEM images of Zn_2SnO_4@N–C composites. The hollow Zn_2SnO_4 boxes without carbon coating is shown in the upper left corner of Fig. 3a. For the original material, the surfaces of the boxes are smooth and edges are flat without other particles agglomeration. For the composites, both the surface and edges become rougher and there are lots of small particles covered on the boxes (Fig. 3a–c), which also can be seen in the SEM images, indicating that the carbon coating is formed by carbon particles. Fig. 3d shows the enlarged edge of boxes, which covered with a thin carbon layer that benecial for mechanical reinforcement and enhancing electronic conductivity of the structure.

The lithium storage capacity and cyclability of anodes in lithium ion cells are determined by the charge/discharge cycling. The comparison of the cycling performance between Zn_2SnO_4@N–C composites, hollow Zn_2SnO_4 boxes and solid Zn_2SnO_4 cubes are carried out, which is shown in Fig. 4a. After 45 cycles, the reversible capacity of hollow Zn_2SnO_4 boxes retains 540 mA h g^{-1} at a current density of 300 mA g^{-1} and the solid Zn_2SnO_4 cubes retain only 395.3 mA h g^{-1}. It indicated that the hollow structure can provide the larger specific surface area, better electrolyte penetration and less inner stress, which can buffer the large volume change and enhance the cycling performance. The rapid fading of Zn_2SnO_4 could be attributed to large volumetric expansion and contraction during Li+ insertion and extraction and low electron conductivity of it. However, the hollow Zn_2SnO_4@C–N composites show a better cycle performance than those two and the discharge and charge capacities are 616 mA h g^{-1} and 598 mA h g^{-1} at the 45th cycle. Fig. 4b shows the rate capability of Zn_2SnO_4@N–C composites which is obtained between 0.01 and 2.0 V at various current densities. When increasing the current density to 600 mA g^{-1}, 800 mA g^{-1}, 1000 mA g^{-1}, 1200 mA g^{-1}, the Zn_2SnO_4@N–C composites still could deliver a discharge (charge) capacity of 490 (475) mA h g^{-1}, 419 (405) mA h g^{-1}, 354 (344) mA h g^{-1}, 297 (287) mA h g^{-1} up to 45 cycles, respectively. This excellent rate performance and cycling performance could result from the two strategies: the hollow inner and N-doped carbon coating, which not only greatly enhances the electric conductivity but also remarkably increases the surface stability of Zn_2SnO_4 boxes and relieves the internal stress volume changes during Li+ insertion/extraction. Fig. 4c shows the EIS analysis of the electrodes of Zn_2SnO_4 boxes and Zn_2SnO_4@N–C composites at 0.5 V from 0.01 Hz to 100 kHz after 45 cycling. The impedance curves consist of one semicircle in the medium frequency region and an inclined line in the low-frequency region. Both the impedance plots can be fitted by the

equivalent circuit diagram. The plots show that the semicircle arc of Zn_2SnO_4@N–C composites is smaller than the Zn_2SnO_4 boxes, which presents a smaller electrochemical reaction resistance due to the N-doped carbon coating layers. Conclusively, the electrode conductivity can be greatly increased by the N-doped carbon adding.

4. Conclusion

In summary, the hollow Zn_2SnO_4@N–C composites are synthesized after the calcined process of precursor 1-methylimidazole. Compared with the solid (hollow) Zn_2SnO_4, the Zn_2SnO_4@N–C composites with a unique hollow structure and N-doped carbon coating exhibit improved structural stability and cycling performance. The hollow interior could provide larger specific surface area, better electrolyte penetration and less inner stress. Additionally, the N-doped carbon layer played an important role for buffering the volumetric change of the boxes, and enhancing the ion and electron conductions. With rational and delicate design, this kind of composites may be the potential anode materials for lithium-ion batteries.

Acknowledgments

This work was supported by the Spaceflight Foundation of the People's Republic of China under Grant no. NBXW0001, the Spaceflight Innovation Foundation of China under Grant no. NBXT0002, the Basic Research Foundation of Northwestern Polytechnical University under Grant no. JC201269 and the Graduate Starting Seed Fund of Northwestern Polytechnical University No. Z2013146.

References

[1] L. Mei, C.C. Li, B.H. Qu, M. Zhang, C. Xu, D. Lei, Small quantities of cobalt deposited on tin oxide as anode material to improve performance of lithium-ion batteries, Nanoscale 4 (2012) 5731.
[2] Z.L. Wang, J.H. Song, Piezoelectric nanogenerators based on zinc oxide nanowire arrays, Science 14 (2006) 242.
[3] M. Armand, J.M. Tarascon, Building better batteries, Nature 451 (2008) 652.
[4] J.M. Tarascon, M. Armand, Issues and challenges facing rechargeable lithium batteries, Nature 414 (2001) 359–367.
[5] X. Wang, X.Q. Cao, L. Bourgeois, H. Guan, S.M. Chen, Y.T. Zhong, D.M. Tang, H.Q. Li, T.Y. Zhai, L. Li, Y. Bando, D. Golberg, N-doped graphene–SnO_2 sandwich paper for high-performance lithium-ion batteries, Advanced Functional Materials 22 (2012) 2682–2690.
[6] J. Xie, X.G. Yang, S. Zhou, D.W. Wang, Comparing One- and two-dimensional heteronanostructures as silicon-based lithium ion battery anode materials, ACS Nano 5 (2011) 9225–9231.
[7] A.S. Arico, P.G. Bruce, B. Scrosati, J.M. Tarascon, W.V. Schalkwijk, Nanostructured materials for advanced energy conversion and storage devices, Nature Materials 4 (2005) 366–377.
[8] Z.Y. Wang, Z.C. Wang, W.T. Liu, W. Xiao, X.W. (David) Lou, Amorphous $CoSnO_3$@C nanoboxes with superior lithium storage capability, Energy & Environmental Science 6 (2013) 87.
[9] Y. Zhao, Y. Huang, Q.F. Wang, X.Y. Wang, M. Zong, Carbon-doped Li_2SnO_3/graphene as an anode material for lithium-ion batteries, Ceramics International 39 (2013) 1741–1747.
[10] Y. Zhao, Y. Huang, Q.F. Wang, Graphene supported poly-pyrrole(PPY)/Li_2SnO_3 ternary composites as anode materials for lithium ion batteries, Ceramics International 39 (2013) 6861–6866.
[11] Q.F. Wang, Y. Huang, J. Miao, Y. Zhao, Y. Wang, Synthesis and electrochemical characterizations of Ce doped SnS_2 anode materials for rechargeable lithium ion batteries, Electrochimica Acta 93 (2013) 120–130.
[12] Q.F. Wang, Y. Huang, J. Miao, Y. Zhao, W. Zhang, Y. Wang, Graphene-supported Ce–SnS_2 nanocomposite as anode material for lithium-ion batteries, Journal of the American Ceramic Society 96 (2013) 2190–2196, http://dx.doi.org/10.1111/jace.12302.
[13] X.H. Xia, J.P. Tu, Y.Q. Zhang, J. Chen, X.L. Wang, C.D. Gu, C. Guan, J.S. Luo, H.J. Fan, Porous hydroxide nanosheets on preformed nanowires by electrodeposition: branched nanoarrays for electrochemical energy storage, Chemistry of Materials 24 (2012) 3793–3799.
[14] P.V. Prikhodchenko, J. Gun, S. Sladkevich, A.A. Mikhaylov, O. Lev, Y.Y. Tay, S.K. Batabyal, D.Y.W. Yu, Conversion of hydroperoxoantimonate coated graphenes to Sb_2S_3@graphene for a superior lithium battery anode, Chemistry of Materials 24 (2012) 4750–4757.
[15] Y.Q. Jiang, C.X. He, R. Sun, Z.X. Xie, L.S. Zheng, Synthesis of Zn_2SnO_4 nanoplate-built hierarchical cube-like structures with enhanced gas-sensing property, Materials Chemistry and Physics 136 (2012) 698–704.
[16] D.W. Kim, S.S. Shin, I.S. Cho, S. Lee, D.H. Kim, C.W. Lee, H.S. Jungd, K.S. Hong, Synthesis and photovoltaic property of fine and uniform Zn_2SnO_4 nanoparticles, Nanoscale 4 (2012) 557–562.
[17] L.L. Li, S.J. Peng, Y.L. Cheah, J. Wang, P.F. Teh, Y. Ko, C. Wonga, M. Srinivasan, Electrospun eggroll-like $CaSnO_3$ nanotubes with high lithium storage performance, Nanoscale 5 (2013) 134–138.
[18] V. Šepelák, S.M. Becker, I. Bergmann, S. Indris, M. Scheuermann, A. Feldhoff, Nonequilibrium structure of Zn_2SnO_4 spinel nanoparticles, Journal of Materials Chemistry 22 (2012) 3117–3126.
[19] Y.J. Chen, B.H. Qu, L. Mei, D. Lei, L. Chen, Q.H. Li, T.H. Wang, Synthesis of $ZnSnO_3$ mesocrystals from regular cube-like to sheet-like structures and their comparative electrochemical properties in Li-ion batteries, Journal of Materials Chemistry 22 (2012) 25373–25379.
[20] K. Kim, A. Annamalai, S.H. Park, T.H. Kwon, M.W. Pyeon, M.J. Lee, Preparation and electrochemical properties of surface-charge-modified Zn_2SnO_4 nanoparticles as anodes for lithium-ion batteries, Electrochimica Acta 76 (2012) 192–200.
[21] W. Song, J. Xie, W.Y. Hu, S.Y. Liu, G.S. Cao, T.J. Zhu, X.B. Zhao, Facile synthesis of layered Zn_2SnO_4/graphene nanohybrid by a one-pot route and its application as high-performance anode for Li-ion batteries, Journal of Power Sources 229 (2013) 6–11.
[22] X.H. Hou, Q. Cheng, Y. Bai, W.F. Zhang, Preparation and electrochemical characterization of Zn_2SnO_4 as anode materials for lithium ion batteries, Solid State Ionics 181 (2010) 631–634.
[23] X.J. Zhua, L.M. Geng, F.Q. Zhang, Y.X. Liua, L.B. Cheng, Synthesis and performance of Zn_2SnO_4 as anode materials for lithium ion batteries by hydrothermal method, Journal of Power Sources 189 (2009) 828–831.
[24] Y. Zhao, Y. Huang, Q.F. Wang, K. Wang, L. Wang, M. Zong, Preparation of hollow Zn_2SnO_4 box for advanced lithium-ion batteries, RSC Advances 34 (2013) 14480–14485, http://dx.doi.org/10.1039/C3RA42176G.
[25] Z.Y. Wang, L. Zhou, X.W. Lou, Metal oxide hollow nanostructures for lithium-ion batteries, Advanced Materials 24 (2012) 1903–1911.
[26] M. Wang, G.D. Li, H.Y. Xu, Y.T. Qian, J. Yang, Enhanced lithium storage performances of hierarchical hollow MoS_2 nanoparticles assembled from nanosheets, Applied Materials & Interfaces 5 (2013) 1003–1008.
[27] T. Song, Y. Jeon, M. Samal, H. Han, H. Park, J. Ha, D.K. Yi, J.M. Choi, H. Chang, Y.M. Choi, U. Paik, A Ge inverse opal with porous walls as an anode for lithium ion batteries, Energy & Environmental Science 5 (2012) 9028.
[28] S. Chaudhari, M. Srinivasan, 1D hollow a-Fe_2O_3 electrospun nanofibers as high performance anode material for lithium ion batteries, Journal of Materials Chemistry 22 (2012) 23049.
[29] W.S. Yuan, Y.W. Tian, G.Q. Liu, Synthesis and electrochemical properties of pure phase Zn_2SnO_4 and composite Zn_2SnO_4/C, Journal of Alloys and Compounds 506 (2010) 683–687.

[30] L. Zhao, Y.S. Hu, H. Li, ZX. Wang, L.Q. Chen, Porous $Li_4Ti_5O_{12}$ coated with N-doped carbon from ionic liquids for Li-ion batteries, Advanced Materials 23 (2011) 1385–1388.

[31] J.S. Lee, X.Q. Wang, H.M. Luo, G.A. Baker, S. Dai, Facile ionothermal synthesis of microporous and mesoporous carbons from task specific ionic liquids, Journal of the American Chemical Society 131 (2009) 4596.

[32] J.S. Lee, X.Q. Wang, H.M. Luo, S. Dai, Fluidic carbon precursors for formation of functional carbon under ambient pressure based on ionic liquids, Advanced Materials 22 (2010) 1004.

[33] J.P. Paraknowitsch, J. Zhang, D.S. Su, A. Thomas, M. Antonietti, Ionic liquids as precursors for nitrogen-doped graphitic carbon, Advanced Materials 22 (2009) 87.